AFRL-RX-WP-TP-2010-4038

ACCURATE CHARACTERIZATION OF FREE CARRIER REFRACTION IN InP (POSTPRINT)

Leonel P. Gonzalez and Shekhar Guha

Survivability Materials Branch
Survivability and Sensor Materials Division

Srinivasan Krishnamurthy

SRI International

FEBRUARY 2010

AIR FORCE RESEARCH LABORATORY
MATERIALS AND MANUFACTURING DIRECTORATE
WRIGHT-PATTERSON AIR FORCE BASE, OH 45433-7750
AIR FORCE MATERIEL COMMAND
UNITED STATES AIR FORCE

REPORT DOCUMENTATION PAGE

Form Approved
OMB No. 0704-0188

1. REPORT DATE *(DD-MM-YY)*	2. REPORT TYPE	3. DATES COVERED *(From - To)*
February 2010	Conference Paper Postprint	01 October 2002 – 01 February 2010

4. TITLE AND SUBTITLE
ACCURATE CHARACTERIZATION OF FREE CARRIER REFRACTION IN InP (POSTPRINT)

5a. CONTRACT NUMBER
In-house

5b. GRANT NUMBER

5c. PROGRAM ELEMENT NUMBER
62102F

6. AUTHOR(S)
Leonel P. Gonzalez and Shekhar Guha (AFRL/RXPJ)
Srinivasan Krishnamurthy (SRI International)

5d. PROJECT NUMBER
4348

5e. TASK NUMBER
RG

5f. WORK UNIT NUMBER
M08R1000

7. PERFORMING ORGANIZATION NAME(S) AND ADDRESS(ES)
Survivability Materials Branch (AFRL/RXPJ)
Survivability and Sensor Materials Division
Materials and Manufacturing Directorate
Wright-Patterson Air Force Base, OH 45433-7750
Air Force Materiel Command, United States Air Force

SRI International
333 Ravenswood Avenue
Menlo Park, CA 94025

8. PERFORMING ORGANIZATION REPORT NUMBER
AFRL-RX-WP-TP-2010-4038

9. SPONSORING/MONITORING AGENCY NAME(S) AND ADDRESS(ES)
Air Force Research Laboratory
Materials and Manufacturing Directorate
Wright-Patterson Air Force Base, OH 45433-7750
Air Force Materiel Command
United States Air Force

10. SPONSORING/MONITORING AGENCY ACRONYM(S)
AFRL/RXPJ

11. SPONSORING/MONITORING AGENCY REPORT NUMBER(S)
AFRL-RX-WP-TP-2010-4038

12. DISTRIBUTION/AVAILABILITY STATEMENT
Approved for public release; distribution unlimited.

13. SUPPLEMENTARY NOTES
Conference paper published in the Proceedings of the SPIE Photonics West Conference, Vol. 7582, held 23 - 28 January 2010, San Francisco, CA. PAO Case Number: 88ABW-2009-5296; Clearance Date: 29 Dec 2009. © 2010 SPIE. The U.S. Government is joint author of this work and has the right to use, modify, reproduce, release, perform, display, or disclose the work. Paper contains color.

14. ABSTRACT
Using recently published results of intrinsic and free carrier nonlinear absorption coefficients in InP, nonlinear refraction was investigated at 1.064 μm using ns duration lasers to characterize refraction from generated free carriers. A phase retrieval algorithm was implemented to determine the amplitude and phase profiles of the incident beam. Accurate spatial and temporal profiles of the incident field were used to model nonlinear propagation through and beyond the sample. With the sample held fixed at focus and the incident energy increased, images of the transmitted beam a fixed distance away were recorded as a function of irradiance. Excellent agreement was observed between recorded beam images and those generated from the numerical model.

15. SUBJECT TERMS
nonlinear optics, infrared, materials

16. SECURITY CLASSIFICATION OF:			17. LIMITATION OF ABSTRACT:	18. NUMBER OF PAGES	19a. NAME OF RESPONSIBLE PERSON (Monitor)
a. REPORT	b. ABSTRACT	c. THIS PAGE			Rafael Reed
Unclassified	Unclassified	Unclassified	SAR	12	19b. TELEPHONE NUMBER *(Include Area Code)* N/A

Standard Form 298 (Rev. 8-98)
Prescribed by ANSI Std. Z39-18

Accurate Characterization of Free Carrier Refraction in InP

Leonel P. Gonzalez[a], Srinivasan Krishnamurthy[b] and Shekhar Guha[a]

[a] Air Force Research Lab, Materials and Manufacturing Directorate, Wright-Patterson Air Force Base, OH 45433;
[b]SRI International, 333 Ravenswood Avenue, Menlo Park, CA 94025

ABSTRACT

Using recently published results of intrinsic and free carrier nonlinear absorption coefficients in InP, nonlinear refraction was investigated at 1.064 μm using ns duration lasers to characterize refraction from generated free carriers. A phase retrieval algorithm was implemented to determine the amplitude and phase profiles of the incident beam. Accurate spatial and temporal profiles of the incident field were used to model nonlinear propagation through and beyond the sample. With the sample held fixed at focus and the incident energy increased, images of the transmitted beam a fixed distance away were recorded as a function of irradiance. Excellent agreement was observed between recorded beam images and those generated from the numerical model.

Keywords: Nonlinear Optics, Infrared, Materials

1. INTRODUCTION

Nonlinear absorption (NLA) in semiconductors is a coupled process where intrinsic two photon absorption (2PA) generates free carriers. For a laser of sufficient temporal duration, the free carriers generated locally modify both the linear absorption and refractive index within the material while the laser pulse is present. Nonlinear refraction (NLR) due to free carriers has long been reported[1] and values for InP obtained using closed aperture Z-scans are in the literature.[2]

As laser pulse durations increase from sub picosecond to nanoseconds or longer, free carrier effects become the dominant NLA and NLR mechanisms. Oftentimes accurate analysis of NLR is hampered by inaccurate knowledge of the spatial amplitude and phase of the incident beam. This has been overcome by use of a phase retrieval method. By capturing images of the incident beam as well as a second image located a known distance away, a method based on the Gerchberg Saxton[3] algorithm has been implemented to retrieve the spatial phase profile of the incident beam. With the amplitude, phase and temporal profile of the incident beam known, the field was numerically modeled through the sample and then propagated a known distance beyond. Both total energy transmission and spatial beam profiles as functions of incident irradiance were recorded and good agreement with the model was observed.

2. THEORY AND NUMERICAL MODELING

2.1 Coupled Nonlinear Beam Propagation and Rate Equations

Equation 1 describes the propagation of the complex electro-magnetic field amplitude, $A(x, y, t)$, through a third order nonlinear medium along the z direction using only the slowly varying amplitude approximation.

$$\frac{\partial A}{\partial z} = \frac{i}{2k_0}\nabla_\perp^2 A + \frac{2i\pi}{\lambda}\left(\sigma_{ref}\Delta N + \frac{dn}{dT}\Delta T + \gamma I\right)A - (\alpha + \sigma_{abs}\Delta N + \beta I)\frac{A}{2} \tag{1}$$

The parameter σ_{ref} is similar to the thermo-optic coefficient, $\frac{dn}{dT}$, and relates the change in refractive index due to generated carriers, $\frac{dn}{dN}$. The instantaneous, or bound electronic, change in the refractive index due to irradiance, I, is given as γ. While included for completeness, since the pulse duration studied here is on the order of nanoseconds, NLR due to γ is much weaker than free carrier refraction effects since the irradiances are relatively low. One and two photon absorption coefficients are α and β respectively and the free carrier absorption cross section is σ_{abs}.

Generated carrier density, $\Delta N(x,y,t)$, and temperature change, $\Delta T(x,y,t)$ are obtained from the following rate equations:

$$\frac{\partial \Delta N}{\partial t} = \frac{\alpha I}{h\nu} + \frac{\beta I^2}{2h\nu} - \frac{\Delta N}{\tau} \quad (2)$$

$$\frac{\partial \Delta T}{\partial t} = \frac{1}{\rho c}\left[(\alpha + \sigma_{abs}\Delta N)I + \beta I^2\right] \quad (3)$$

The carrier recombination lifetime τ is much longer than the pulse duration used here. The density is ρ while c denotes the specific heat of the medium. The 2PA coefficient, β, and the free carrier absorption cross section, σ_{abs} are temperature dependent parameters.[4] A paper detailing the theory and temperature dependent β and σ_{abs} parameters for InP is in preparation.

2.2 Numerical Method

To model the propagation of an electro magnetic field through the sample, Eq. (1) is numerically solved via the operator splitting method.[5] The right side of the equation is separated into linear and nonlinear operations which are solved independently. First the sample length is divided into a number of slices of length Δz. Both the amplitude and phase of the incident field $A(x,y,t)$ at $z = Z_1$ are known from the experimental conditions and transmission losses are accounted for to determine the field just inside the sample. Next, with the nonlinearities turned off, diffraction over a distance $\frac{\Delta z}{2}$ is solved for each time slice by use of the two dimensional fast Fourier transform beam propagation method (FFT-BPM).[6,7] Then diffraction is set to zero and the rate equations are solved at this z location via finite difference approximations. Updated values for $\Delta N(x,y,t)$ and $\Delta T(x,y,t)$ are used to modify the electric field. Lastly the field is propagated $\frac{\Delta z}{2}$ and the process is repeated until the pulse reaches the end of the sample. At the exit of the sample the field is modified by the transmission coefficient and is temporally and spatially integrated to calculate the output energy. Using the FFT-BPM allows propagation of the field at the exit of the sample to any measurement plane after the sample. Each time slice of the field is propagated and then temporally integrated to determine a fluence distribution for comparison with the camera image recorded at the same plane.

2.3 Determination of the Incident Amplitude and Phase

To determine the incident spatial field, $A(x,y,z = Z_1,t)$, a phase retrieval method similar to Pandey et al.[8] was used but with the addition of a discrete wavelet transform (DWT). Beam images at two locations, the sample input plane, Z_1, and the detector plane, Z_2, were recorded. After background corrections, the square root of the beam images are taken to determine the field amplitudes at each plane. An initial guess is taken for the phase at Z_1 and the complex amplitude is then propagated to Z_2. The phase and amplitude are separated and the resulting propagated amplitude is replaced with the known amplitude. A DWT is used on the retrieved phase to filter and smooth the data and minimize noise effects. A complex field at Z_2 based on the original known amplitude and retrieved, filtered phase is back propagated to Z_1. This process is repeated until the errors are below a preset threshold value. To verify the accuracy of the retrieved phase, the field is propagated to a third plane beyond Z_2 and compared with the recorded beam image there.

The incident temporal distribution of $A(x,y,t)$ was measured using a fast photodiode and oscilloscope (4 GHz). The pulse shape was normalized and a cubic spline used to decrease the number of sampling points while not losing any temporal features. The final number of time points sets the number of time slices in the simulated amplitude.

3. RESULTS AND ANALYSIS

3.1 Experimental Layout

The experimental set-up shown in Fig. 1 consists of a flashlamp pumped, electro-optically q-switched Nd:YAG laser at 1.064 μm (Quantel Brilliant) with a pulse duration of 3.7 ns (FWHM). No spatial filtering of the beam was done. The beam was sent though a half wave plate and polarizer for attenuation. The half wave plate was mounted on a computer controlled rotation stage. Next the beam was reflected by a 45° partial reflector. The

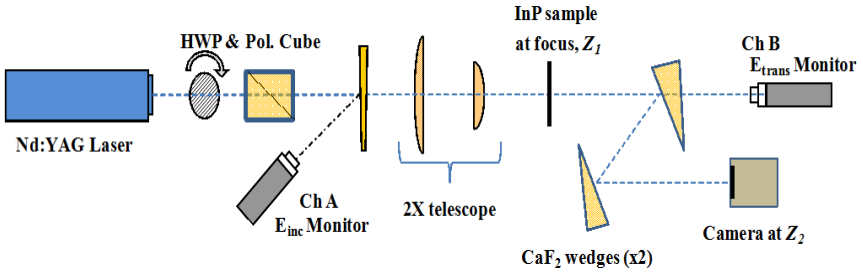

Figure 1. Experimental layout

transmitted beam was sent to a pyroelectric detector used to monitor the incident energy (Ch. A detector in Fig. 1). Next a $2X$ down telescope was used to increase the irradiance at the sample. The beam was loosely collimated after the down telescope to ensure that the sample thickness was thin compared to the diffraction distance of the beam. The irradiance scan method[9] was used where the sample was kept fixed at focus while the incident energy was varied.

A pair of CaF_2 wedges were placed immediately after the sample. The front surface reflections from the wedges were sent to a camera located at Z_2 while the transmitted beam energy through the first wedge was measured by a second pyroelectric energy detector (Ch. B). The distance between planes Z_1 and Z_2 was 650 mm with Z_2 located within the Rayleigh range of the beam. Placing the detector in the near field maximizes the amount of observed signal due to NLR. If the detector is placed in the far field, less NLR effects are observed since linear diffraction due to free space propagation will dominate.

3.2 Nonlinear Absorption Results

Figure 2 shows the nonlinear transmission measured as the ratio of detectors B/A as a function of incident energy.

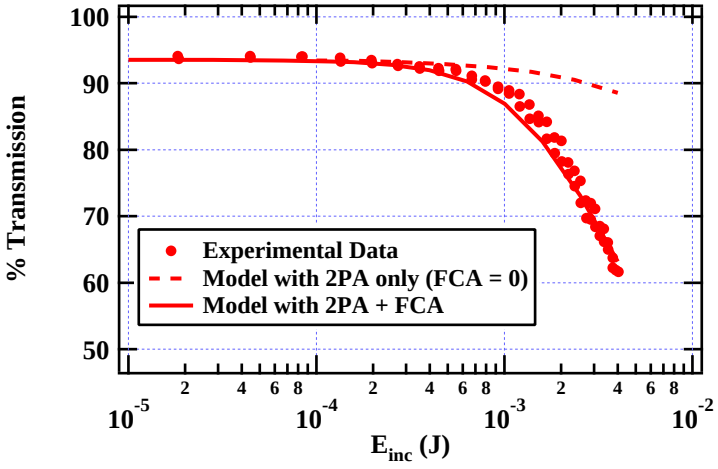

Figure 2. Nonlinear absorption in InP at 1.064 μm using nsec pulses.

In Fig. 2 the circles are experimental data, dashed line is numerical modeling results using only 2PA and solid line is modeling results including both 2PA + FCA. The InP sample was 1.0 mm thick and was anti-reflection coated. The incident beam was elliptical and approximately Gaussian. Fitting a Gaussian to the beam irradiance gives 1/e radii of 1.0 and 0.5 mm in the horizontal and vertical directions. The pulse width was 2.8 nsec FWHM. The values of $\beta = 25.5$ cm/GW and $\sigma_{abs} = 1.5 \times 10^{-17}$ cm^2 were used in the numerical modeling.[10]

3.3 Nonlinear Refraction Results

Measurement of nonlinear refraction was done by recording camera images at plane Z_2 as a function of the incident irradiance. Figure 3 shows the beam recorded at Z_2 (left) and the result of the numerical model (center)

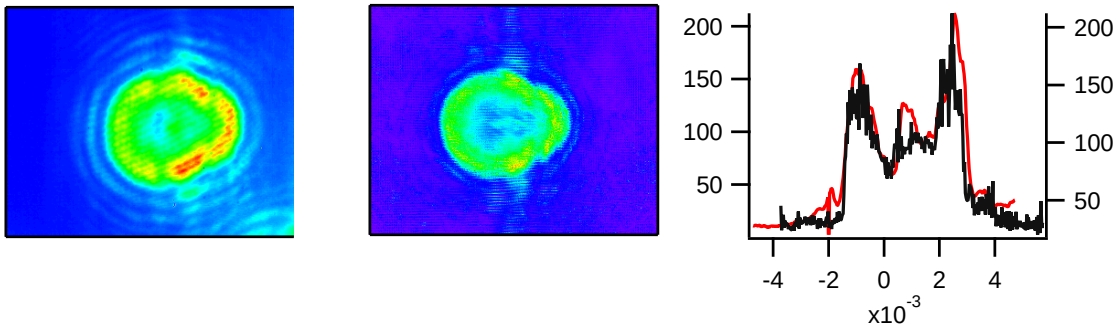

Figure 3. Beam images from camera (left) and modeling results (center) at plane Z_2 for incident irradiance of 79 MW/cm^2. Right column shows a comparison of the horizontal line profiles through the centers of both images.

for an incident irradiance of 79 MW/cm^2. The graph (right) shows a horizontal line profile through the center of both images. The free carrier refraction coefficient was determined by iteratively adjusting the value of the parameter while minimizing the errors between the recorded images and numerical result over all irradiances. Note that the beam images from the camera and model are not on the same intensity scale.

4. CONCLUSION

With recently published results of intrinsic and free carrier nonlinear absorption coefficients in InP, nonlinear refraction was investigated at 1.064 μm using ns duration lasers in order to characterize refraction from generated free carriers. A phase retrieval algorithm was implemented to determine the amplitude and phase profiles of the incident beams. Accurate spatial and temporal profiles of the incident beams were used to model nonlinear propagation through the sample and linear propagation beyond. With the sample held fixed at focus, images of the transmitted beam a fixed distance away were recorded as a function of incident irradiance. Excellent agreement was observed between recorded beam images and those generated from the numerical model.

REFERENCES

[1] Said, A. A., Sheik-Bahae, M., Wei, T. H., Young, J., and Van Stryland, E. W., "Determination of bound-electronic and free-carrier nonlinearities in ZnSe, GaAs, CdTe, and ZnTe," *J. Opt. Soc. Amer. B* **9**(3), 405–414 (1992).

[2] Dvorak, M. D. and Justus, B. L., "Z-scan studies of nonlinear absorption and refraction in bulk, undoped InP," *Opt. Comm.* **114**(1-2), 147–150 (1995).

[3] Gerchberg, R. W. and Saxton, W. O., "A prectical algorithm for the determination of phase from image and diffraction plane pictures," *Optik (Stuggart)* **35**, 237–246 (1972).

[4] Krishnamurthy, S., Yu, Z. G., Gonzalez, L. P., and Guha, S., "Accurate evaluation of nonlinear absorption coefficients in InAs, InSb, and HgCdTe alloys," *J. Appl. Phys.* **101**(11), 113104 (2007).

[5] Burzler, J. M., Hughes, S., and Wherrett, B. S., "Split-step Fourier methods applied to model nonlinear refractive effects in optically thick media," *Appl. Phys. B* **62**(4), 389–397 (1996).

[6] Feit, M. D. and Fleck, J. A., J., "Light propagation in graded-index optical fibers," *Appl. Opt.* **17**(24), 3990 (1978).

[7] Agrawal, G. P., [*Nonlinear Fiber Optics*], Academic Press, New York, 4th ed. (2007).

[8] Pandey, A. R., Haus, J. W., Powers, P. E., and Yaney, P. P., "Optical field measurements for accurate modeling of nonlinear parametric interactions," *J. Opt. Soc. Amer. B* **26**(2), 218–227 (2009).

[9] Gonzalez, L. P., Murray, J. M., Cowan, V. M., and Guha, S., "Measurement of the nonlinear optical properties of semiconductors using the Irradiance Scan technique," *Nonlinear Frequency Generation and Conversion: Materials, Devices, and Applications VII* **6875**(1), 68750R, SPIE (2008).

[10] Gonzalez, Leonel, P., Murray, J. M., Krishnamurthy, S., and Guha, S., "Wavelength dependence of intrinsic and free carrier nonlinear absorption in InP," *Opt. Exp.* **17**(11), 8741–8748 (2009).